

Application of the MAX/EGS4 exposure model to the dosimetry of the Yanango radiation accident

R. Kramer¹, A. M. Santos¹, C. A. O. Brayner¹, H. J. Khoury¹, J. W. Vieira², F. R. A. Lima³

¹Departamento de Energia Nuclear, UFPE, Recife, PE, Brazil

²Centro Federal de Educação Tecnológica de Pernambuco, Recife, PE, Brazil

³Centro Regional de Ciências Nucleares, CNEN, Recife, PE, Brazil

E-mail: rkramer@uol.com.br

Statement of provenance:

‘This is an author-created, un-copyedited version of an article accepted for publication in Physics in Medicine and Biology. IOP Publishing Ltd is not responsible for any errors or omissions in this version of the manuscript or any version derived from it. The definitive publisher authenticated version is available at [doi:10.1088/0031-9155/50/0/000](https://doi.org/10.1088/0031-9155/50/0/000). ‘

ABSTRACT

According to the International Atomic Energy Agency (IAEA), industrial radiography accounts for approximately half of all reported accidents for the nuclear related industry. Detailed information about these accidents has been published by the IAEA in its Safety Report Series, one of which describes the radiological accident which happened in 1999 in Yanango/Peru. Under unsettled circumstances a ¹⁹²Ir source was lost from an industrial radiographic camera and later picked up by a welder, who normally had nothing to do with the radiographic work. The man put the source into the right back pocket of his jeans and continued working for at least another 6.5 hours.

This study uses the MAX/EGS4 exposure model in order to determine absorbed dose distributions in the right thigh of the MAX phantom, as well as average absorbed doses to radiosensitive organs and tissues. For this purpose the Monte Carlo code for standard exposure situations has been modified in order to match the irradiations conditions of the accident as closely as possible. The results present the maximum voxel absorbed dose, voxel depth absorbed dose and voxel surface absorbed dose distributions, average organ and tissue doses, and a maximum surface absorbed dose for zero depth.

1. Introduction

The history of the beneficial use of ionising radiation by medicine and industry represents also the history of its accidents. At first the lack of knowledge about the deleterious effects caused by ionizing radiation was a major contributing factor to the occurrence of overexposures, whereas today human and technical failure represents the main causes. According to the International Atomic Energy Agency (IAEA), “industrial radiography accounts for approximately half of all reported accidents for the nuclear related industry, in both developed and developing countries.” (IAEA1998a).

Appropriate medical care for victims of radiological accidents depends very much on a reliable assessment of the organ and tissue absorbed doses received. The IAEA states:”The prognosis and medical handling of individuals exposed to external radiation depend upon whether the whole body has been exposed, or whether exposure has been localized. It is very important for the prognosis and choice of treatment to know how the absorbed dose has been distributed within the body. Physical dosimetry is very important, since no appropriate biodosimetric method is available for the early stages of local radiation injury.” (IAEA 1998b).

Information on radiological accidents is frequently published by the IAEA in its Safety Report Series with details about the exposure conditions, which are useful for the simulation of the accident with an appropriate exposure model.

The recently introduced MAX/EGS4 exposure model (Kramer et al 2003) has until now mainly been used to determine conversion coefficients between effective dose and operational quantities to be applied to practices well below the dose limits set for routine radiation protection (Kramer et al 2004, 2005a,b,c, Lima et al 2005). For this purpose absorbed doses have been averaged over the volumes of organs and tissues of interest according to the concept of effective dose as defined by the International Commission on Radiological Protection (ICRP 1991).

In case of radiological accidents, especially for highly non-uniform irradiations, one has to determine the maximum absorbed dose in the body, and the absorbed dose distribution in the vicinity of the maximum in order to provide reasonable dosimetric data for the medical treatment of the exposed person(s).

Having a voxel structure with a fine spatial resolution, the MAX phantom lends itself to the purpose of accidental dosimetry, and the EGS4 Monte Carlo code is sufficiently fast to allow for the calculation of the mean absorbed dose per voxel, hereafter called voxel absorbed dose, with a small coefficient of variance in a reasonably short execution time. In order to put the MAX/EGS4 exposure model to the test a radiological accident with a highly non-uniform external exposure of the victim was chosen.

The accident occurred on February 20, 1999 at the Yanango hydroelectric power plant in Peru when a welder, who normally had nothing to do with the radiographic work, picked up a 1.37 TBq ¹⁹²Ir industrial source and put it into the right back pocket of his jeans, where it remained for at least 6.5 hours. For 3 hours the welder was sitting while working inside a 2m diameter tube, and for 3.5 hours he was standing.

The report of the IAEA on the accident (IAEA 2000) provides the following information on the dosimetry:

- a) Using a Prowess 3000 treatment planning computer system a Peruvian physicist of the Instituto Nacional de Enfermedades Neoplásicas (INEN) performed depth dose calculations three days after the accidents. Table 1 shows the results of these calculations.

Table 1. Distribution of doses by depth as calculated by the Instituto Nacional de Enfermedades Neoplásicas (INEN) taken from IAEA (2000)

Organ	Distance (cm)	Dose (Gy)
Skin	1	9966
Soft tissue	2	2508
Soft tissue	3	1110
Soft tissue	4	617
Soft tissue	5	388
Soft tissue	6	265
Soft tissue	7	191
Femur	8	143
Femoral artery	8	143
Soft tissue	9	111
Soft tissue	10	88
Gonads	18	23
Bladder	20	18
Rectum	20	18
Thyroid	90	-

- b) Later physical dosimetry assessment was performed in France based on Monte Carlo techniques, apparently based on methods developed by Roux et al (2000, 2001). As for the assumptions made concerning the source geometry the IAEA report states: “It was assumed that the source was a cylinder, 4 mm in diameter and 8 mm long, enclosed in a steel capsule, 1 mm thick and 1.2 cm long. Two source-skin distances were considered: 3 mm corresponding to the man sitting, and 7 mm (due to the loose fitting jeans) when the man was standing.”

As for the Monte Carlo results the IAEA report continues:

“Normalization of the results was performed on the dose value at the rim of the lesion, which was estimated to be around 25 Gy with an uncertainty of about 30%. On the basis of these assumptions and calculations, taking a lesion of 10 cm diameter, the 100 Gy isodose at the surface of the skin would be located between 2 and 3 cm from the center of the lesion..... The estimated dose to the femur varied from 15 Gy at the entrance to 5 Gy at the exit.” And finally: “These estimated doses were significantly different from those estimated in Peru.”

- c) A whole body dose of ca. 1.25 Gy has been determined with biological dosimetry, however this result has to be considered with caution because the blood sample was taken only on day 106 after exposure and the use of several blood transfusions during the treatment of the patient.

The purpose of this study is to demonstrate that the MAX/EGS4 exposure model can be used for the simulation of radiological accidents. As for the special case under consideration, the results will give an assessment of the maximum absorbed dose in the center of the lesion, isodoses into the depth and on the surface, and also average organ and tissue absorbed doses.

2. Materials and Methods

2.1 The MAX/EGS4 exposure model

The MAX phantom has been developed by Kramer et al (2003) based on segmented CT images (Zubal et al 1994). Its matrix consists of cubic voxels of 3.6mm length. After segmentation the volumes of radiosensitive organs and tissues have been adjusted in order to match the reference masses defined by ICRP89 (ICRP 2003). The phantom has a heterogeneously structured skeleton with voxel-specific skeletal tissue compositions based on masses, percentage distributions, and cellularity factors from ICRP70 (ICRP 1995). A detailed description of the voxel phantom is given in Kramer et al (2003).

The EGS4 Monte Carlo code (Nelson et al 1985) simulates coupled electron-photon transport through arbitrary media. The default version of EGS4 applies an analogous Monte Carlo method, which was used for the calculations of this investigation. Rayleigh scattering has been taken into account, and secondary electrons have been transported down to a cut-off energy of 200 keV.

2.2 Exposure parameters

2.2.1 Source geometry

During disintegration ¹⁹²Ir parent and daughter nuclei emit photons and electrons. For an unshielded source table 2 shows the most important energies and frequencies of the emitted gamma and beta particles which have been taken from data compiled by Delacroix et al (2002). The average energies have been calculated and added to the table.

Table 2. Gamma and Beta energy distributions for an unshielded ^{192}Ir source (Delacroix et al 2002)

Ir-192	Gamma		Beta	
	E (keV)	Frequency	E (keV)	Frequency
E1	317	83	256	6
E2	468	48	536	41
E3	604	8	672	48
Average	372		583	

Figure 1 shows the real ^{192}Ir source which “was a cylinder, 4 mm in diameter and 8 mm long, enclosed in a steel capsule, 1 mm thick and 1.2 cm long” (IAEA 2000), and also the source simulated in the Monte Carlo calculations, which was a parallelepiped with dimensions of 3.6mm x 3.6mm x 7.2mm.

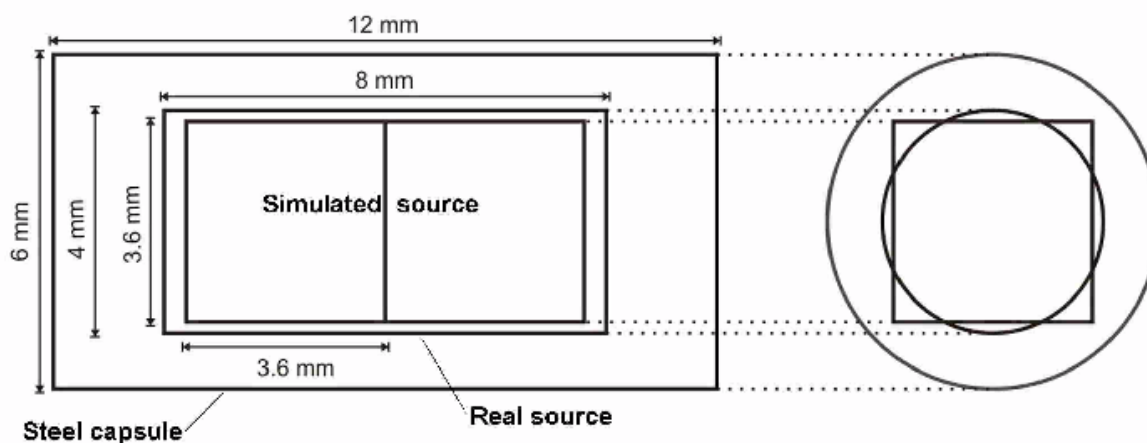


Figure 1. Real ^{192}Ir source with steel capsule according to IAEA (2000) and simulated source of the MAX/EGS4 calculations.

The CSDA range of a 700 keV electron in iron is ca. 0.5mm, which means that the beta particles, because of their energies shown in table 2, are shielded by the steel capsule, and therefore have not been taken into account for the Monte Carlo calculations. Bremsstrahlung released from the slowing down of the beta particles in the steel capsule can also be neglected, because for 700 keV electrons the ratio between radiative and total stopping power in iron is about 0.023 (Hubbell and Seltzer 1996), and especially for sealed ^{192}Ir sources Borg and Rogers (1999) found contributions of Bremsstrahlung to the air kerma strength to be well below 0.5%. In the Monte Carlo calculations the energies of the gamma particles have been sampled from the distribution given in table 2. Initial directions of the photons have been sampled isotropically, and it is assumed that photoelectric absorption and Compton scattering inside the ^{192}Ir source would not change significantly the isotropic distribution of the photons leaving the source, i.e. that only a fraction of the total number of photons emitted from the source in fact reaches the surface of the MAX phantom.

For the average gamma energy of 372 keV, using the exponential attenuation law, one can calculate that the steel capsule would reduce the number of photons leaving the ^{192}Ir source by ca. 8%. Because of the voxel dimensions of 3.6mm it was not possible to simulate the steel capsule, unless one would make a resampling of the whole MAX matrix to reach a 1mm voxel resolution. Although possible, this procedure would increase memory requirements and execution time significantly. Therefore the attenuation effect of the steel capsule was taken into account after the Monte Carlo calculation, by reducing the calculated maximum absorbed dose by 8%, thereby assuming that for given exposure conditions the absorbed dose is basically proportional to the number of photons. This assumption holds if the gamma spectrum would not be changed significantly by the steel capsule.

Indeed, investigations made with spectra available for industrial radiography sources including a steel capsule showed that the average energy of the gamma particles was ca. 386 keV, which differs less than 4% from the average gamma energy of 372 keV for the unshielded source.

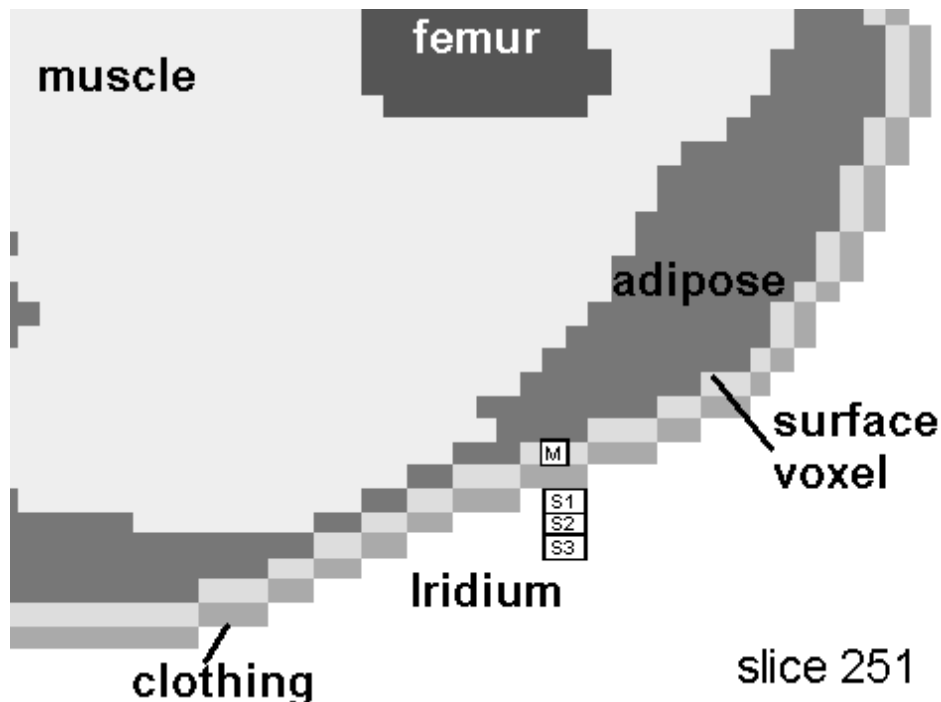


Figure 2. Part of the thigh of the MAX phantom with the ^{192}Ir source for three different source-to-surface distances (SSDs). S1: SSD = 5.4mm, S2: SSD = 9.0mm, S3: SSD = 12.6mm. M = Location of the maximum voxel absorbed dose.

The simulated source differs only slightly from the real source with respect to the form, and the volume of the parallelepiped is only 7% smaller than that of the cylinder. Therefore it is not to be expected that the differences of form and volume between the real and the simulated source would have a significant impact on the number and on the energy distribution of the photons leaving the source.

Figure 2 shows a part of slice 251 of the thigh of the MAX phantom where the ^{192}Ir source was located horizontally in front of the back side close to the surface. The exact orientation of the source was not reported in the IAEA report, but because of its small size this lack of information is not considered to be critical for the absorbed dose distribution inside the body. The body is surrounded by a voxel layer, which represents the cotton clothing (jeans + underwear) of the person who suffered the accident. Elemental composition and density of the cotton material was provided by the National Institute of Standards and Technology (NIST 2005).

If one takes the center of a source voxel as reference point, then the three source-to-surface distances (SSDs) to be simulated in the Monte Carlo runs are:

$$\text{SSD1} = 3.6\text{mm cotton} + 1.8\text{mm source} = 5.4\text{mm}$$

$$\text{SSD2} = 3.6\text{mm cotton} + 3.6\text{mm air} + 1.8\text{mm source} = 9.0\text{mm}$$

$$\text{SSD3} = 3.6\text{mm cotton} + 7.2\text{mm air} + 1.8\text{mm source} = 12.6\text{mm}$$

The Monte Carlo results for these SSDs will provide the data necessary for the calculation of the maximum voxel absorbed dose for a SSD = 3.6mm by extrapolation, and for a SSD = 7mm by interpolation, respectively. (A SSD = 3.0mm cannot be realized when the body is covered by a 3.6mm voxel layer of clothing).

2.2.2 Regions of interest

The MAX phantom stands inside a parallelepiped with 158 columns \times 74 rows \times 487 slices = 5694004 voxels. Monte Carlo calculations for average organ and tissue absorbed doses can be executed very fast with the MAX/EGS4 exposure model, because energy deposition, summation and statistics have to be performed by the algorithm for only 40 different organ and tissue volumes. Calculating the maximum voxel absorbed dose, and doing all Monte Carlo accounting and the statistics for more than 5.5 million voxels would require enormous execution times, wherefore it turned out to be necessary to define certain regions of interests (ROIs). Depending on the dosimetric quantity to be calculated a ROI has to be defined with respect to the maximum acceptable numbers of columns, rows and slices in order to get the calculation done in a reasonable amount of time. The Monte Carlo code transports the particles through all voxels, but it considers only voxels within the ROI when it comes to accounting, statistics and dose calculation.

For the simulation of the Yanango radiological accident, apart from the maximum voxel absorbed dose, the dose distribution into the depth of the thigh and the dose distribution on the surface of the thigh had to be determined. Therefore these calculations were done with two different ROIs:

For the calculation of the depth dose distribution a ROI1 of 17080 voxels has been taken into account, which was made of 5 adjacent slices, in each of which an area of ca. 20cm \times 20cm has been considered.

For the calculation of the surface dose distribution a ROI2 of 51471 voxels has been taken into account, which was made of 57 slices, in each of which an area of ca. 15cm \times 7cm has been considered.

3. Results and discussion

Based on the source geometry and the ROIs described in the previous section, the MAX/EGS4 Monte Carlo code has been modified in order to calculate the voxel absorbed dose distributions in the selected ROIs for the two-voxel ^{192}Ir source located in slice 251 at the positions S1, S2, and S3 shown in figure 2. Four runs have been made with 20 million primary photons each: three runs with SSDs = 5.4mm, 9.0mm, and 12.6mm for ROI1, and one run with SSD = 5.4mm for ROI2 with the MAX phantom always standing, a posture which obviously has also been used throughout all IAEA calculations.

3.1 The maximum voxel absorbed dose

Taking into account 2.2 emitted photons per disintegration the Monte Carlo simulations calculated the following maximum voxel absorbed doses per cumulated activity D_{max} (SSD) as function of the SSD together with the coefficients of variance (C.V.):

$$D_{\text{max}} (5.4\text{mm}) = 3.89 \times 10^{-10} \text{ mGy / Bq s} \quad \text{C.V.} = 1.31\%$$

$$D_{\text{max}} (9.0\text{mm}) = 1.82 \times 10^{-10} \text{ mGy / Bq s} \quad \text{C.V.} = 1.91\%$$

$$D_{\text{max}} (12.6\text{mm}) = 1.11 \times 10^{-10} \text{ mGy / Bq s} \quad \text{C.V.} = 2.45\%$$

The maxima for SSD = 5.4mm and for 9.0mm were found in slice 251 in a surface voxel facing the source, shown in figure 2 by the label "M", whereas the maximum for SSD = 12.6mm was found in slice 253 in a surface voxel diagonal to the right in front of the source at a distance of ca. 5.1mm from the source.

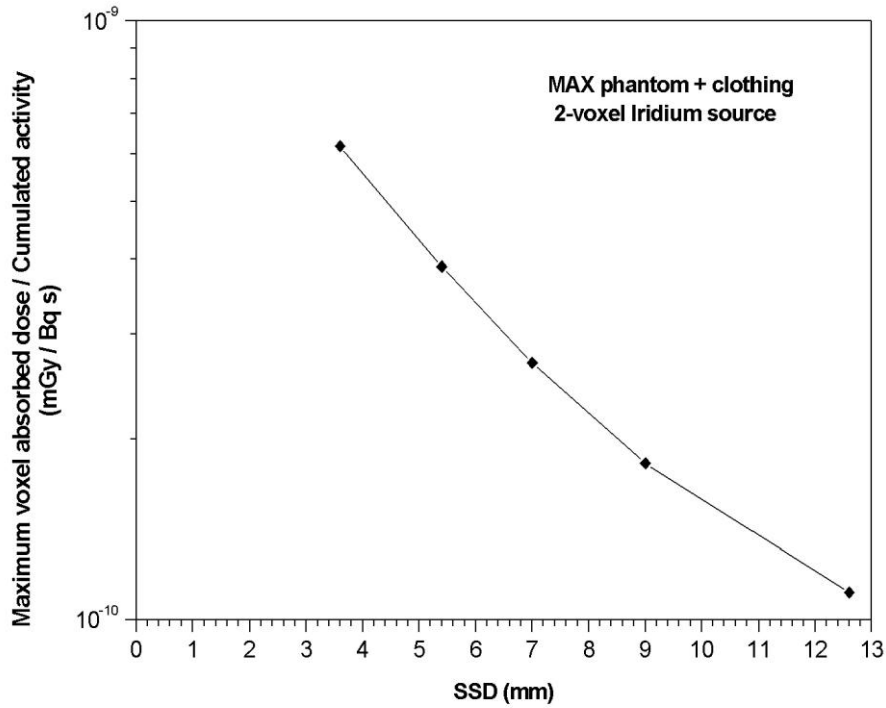


Figure 3. Maximum voxel absorbed dose per cumulated activity as a function of the source-to-surface distance (SSD). Value for 3.6mm extrapolated, value for 7.0mm interpolated.

Figure 3 shows these three maxima plotted as a function of the SSD. With an appropriate exponential fit the values for SSD = 3.6mm, and for SSD = 7mm have been determined by extrapolation and by interpolation, respectively, as

$$D_{\max}(3.6\text{mm}) = 6.19 \times 10^{-10} \text{ mGy / Bq s}$$

$$D_{\max}(7.0\text{mm}) = 2.68 \times 10^{-10} \text{ mGy / Bq s}$$

Taking into account the shielding by the steel capsule, the exposure time, the proportion of time spent sitting and standing, and the total activity of the source, the resultant maximum voxel absorbed dose D_{\max} can be calculated as:

$$\begin{aligned} D_{\max} &= 0.92 \times 6.5 \text{ h} \times 1.37 \times 10^{12} \text{ Bq} \times \{(3.0/6.5) \times D_{\max}(3.6\text{mm}) + (3.5/6.5) \times D_{\max}(7.0\text{mm})\} \\ &= 12683 \text{ Gy} \end{aligned}$$

at a depth of 1.8mm in the surface voxel “M” shown in figure 2 with a C.V. between 1.0% and 1.5%.

3.2 Depth dose distributions

The distribution of the absorbed dose as a function of the depth in the thigh was the result of two irradiations, one with a SSD = 3.0mm, and another one with a SSD = 7.0mm, which also can be considered as having been caused approximately by only one irradiation with a SSD = $[(0.462 \times 3^2 + 0.538 \times 7^2)]^{1/2} = 5.5\text{mm}$, taking the relative exposure times, 3.0/6.5 and 3.5/6.5, also into account.

The Monte Carlo calculation performed with a SSD = 5.4mm, produced approximately the required dose distribution as a function of the depth.

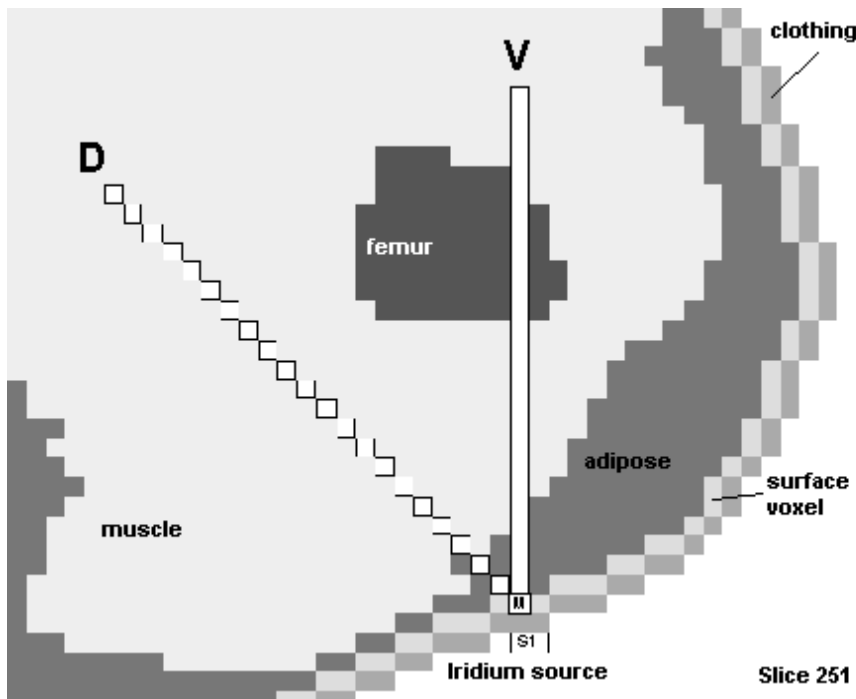


Figure 4. Representation of the vertical (V) and the diagonal (D) depth dose. M = maximum voxel absorbed dose, S1 = ^{192}Ir source at SSD = 5.4mm

According to figure 4 a vertical and a diagonal depth dose have been determined. The vertical depth dose is shown in figure 5 with diamonds. With respect to the maximum absorbed dose of 12683 Gy at 1.8mm depth, the percentage depth doses are 14% at 10mm, 4% at 30mm, 1.6% at 50mm, and 0.7% at 80mm. The C.V.s are smaller than 6% up to 30mm depth, smaller than 10% up to 50mm depth, and smaller than 20% up to 100mm depth.

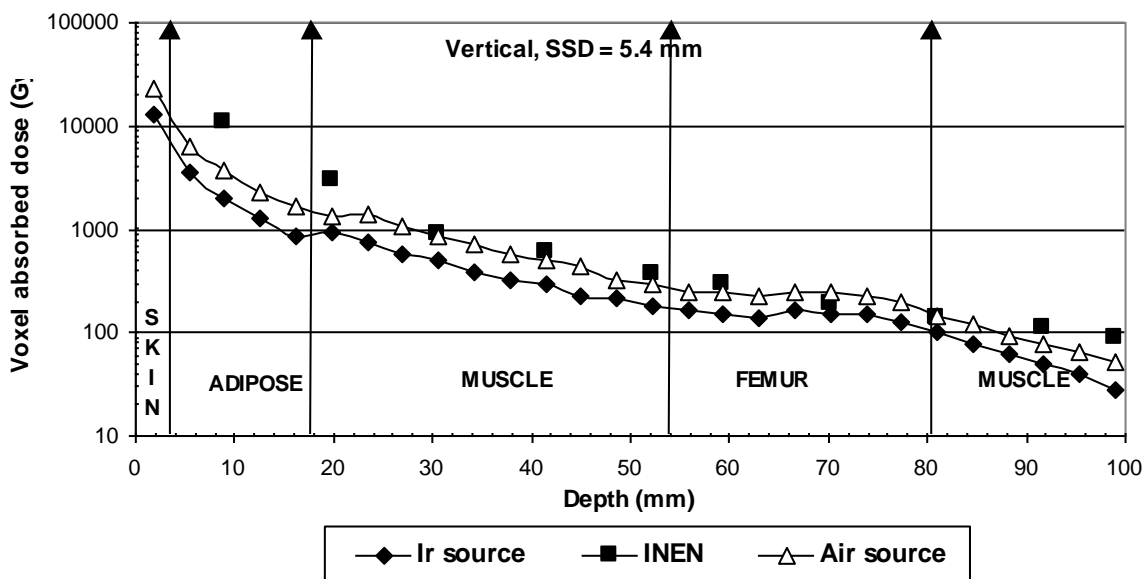


Figure 5. Vertical voxel absorbed dose as a function of the depth for SSD = 5.4mm for a two-voxel ^{192}Ir source, for a two-voxel air source, and for the depth dose data reported by the INEN.

At the entrance of the femur the absorbed dose is ca. 178 Gy, and at the exit side ca. 101 Gy, values which are more than ten times greater than the corresponding doses reported for the Monte Carlo calculations quoted in the IAEA report, but whose average value of 140 Gy on the other hand compare well with the average femur absorbed dose of 143 Gy reported by the INEN in table 1. For photon energies below 200 keV the absorption of energy in bone is usually significantly greater than in muscle. However, in the case considered here, especially in the part where the photons enter the femur, they have energies still well above 200 keV, which is reflected by the relatively smooth transition of the depth dose across the femur.

Figure 5 shows for comparison also the INEN data from table 1 with squares, although these data refer to a different phantom and to different irradiation conditions. For example, the location of the femur is at 8cm depth for the INEN data, while the center of the femur of the MAX phantom is at 6.7cm depth. In general the INEN depth doses are significantly greater than the MAX/EGS4 depth doses calculated with the two-voxel iridium source. The IAEA report on the Yanango radiological accident gives no information about the irradiation conditions chosen by the Peruvian physicist when he made the depth dose calculation with the therapy treatment planning software. Therefore it was assumed that the Peruvian physicist simulated an unshielded point source close to the skin emitting only photons with an average energy of 372 keV, and that he took some shielding by the clothing into account. These conditions, which would use air instead of iridium inside the two-voxels source, and neglect the shielding by the steel capsule, have been simulated with the MAX/EGS4 code. The result is shown in figure 5 by the curve with triangles, which agrees with the INEN data at least for depths between 3 cm and 9 cm. The absorbed dose differences between the curves for the iridium source and the air source are due to attenuation of the emitted photons within the iridium, which is almost three times heavier than iron, and also in the steel capsule. Figure 6 shows the diagonal depth dose which is not significantly different from the vertical depth dose, thereby confirming an almost isotropic dose distribution.

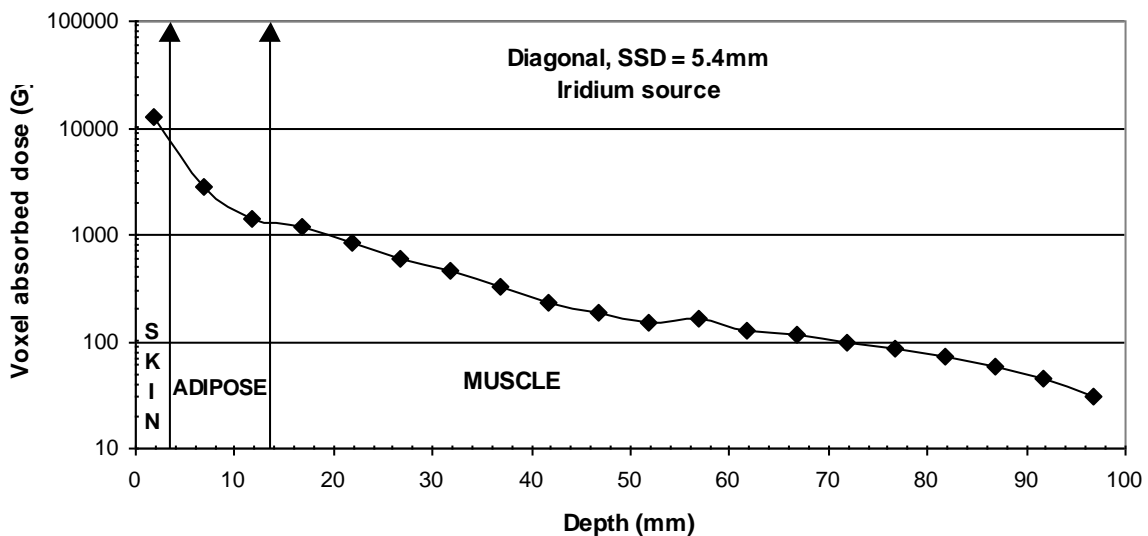


Figure 6. Diagonal voxel absorbed dose as a function of the depth for SSD = 5.4mm for a two-voxel ^{192}Ir source

Figure 7 visualizes the isodose distribution in slice 251. Confirming figures 5 and 6, the isodoses show a rapid decrease of the absorbed dose as a function of depth, but because of the extreme exposure conditions the 1 to 10% isodose range still represents absorbed doses between 127 and 1268 Gy.

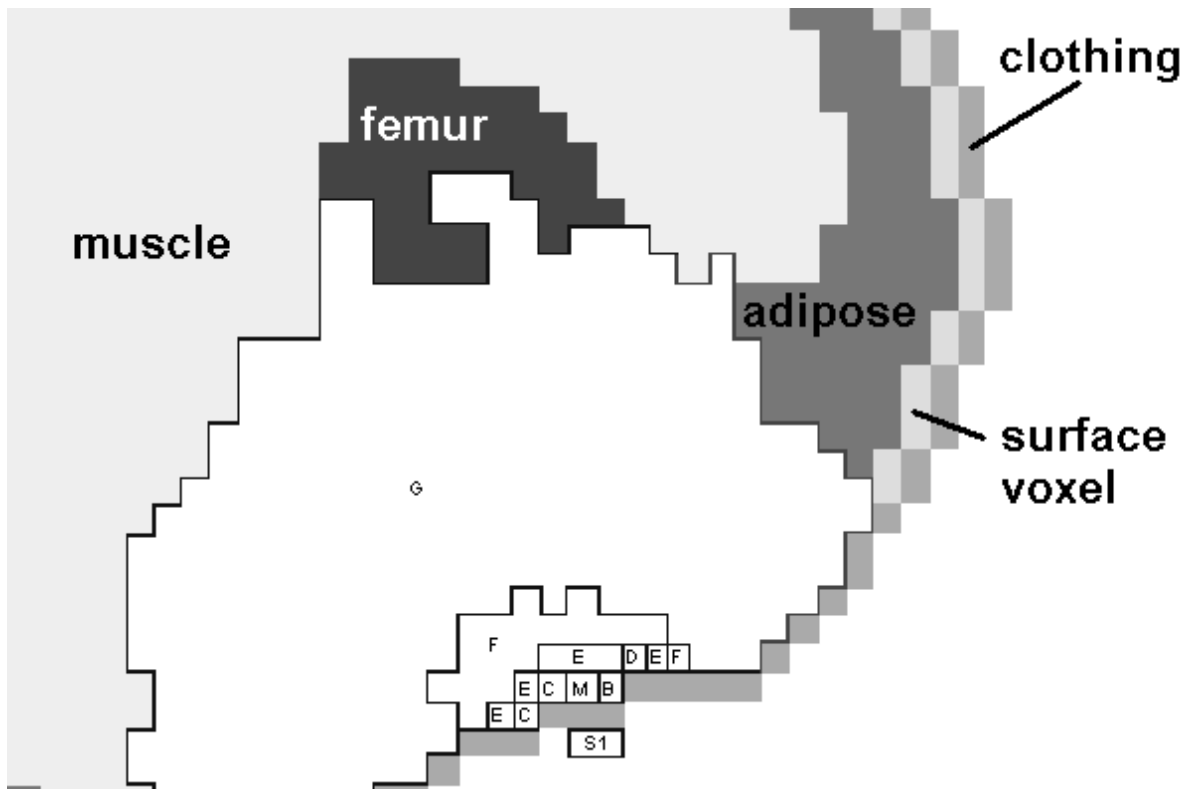


Figure 7. Depth isodoses in the thigh for the absorbed dose distribution with SSD = 5.4mm
M = maximum voxel absorbed dose, Isodoses: B = 99%, C = 65-70%, D = 35%, E = 20-30%
F = 10-20%, G = 1-10%, S1 = ¹⁹²Ir source

3.3 Surface dose distribution

Calculations for the ROI2 produced among other quantities the relative absorbed doses in the surface voxels (= voxel absorbed dose divided by the maximum voxel absorbed dose) of slices 223 – 279. This range corresponds to a distance of 20cm with the source slice 251 being at the center at 10cm. On the 100 Gy isodose for SSD = 5.4mm the relative absorbed dose in a surface voxel at 1.8mm depth is $100 \text{ Gy} / 12683 \text{ Gy} = 0.008$. The output of the Monte Carlo calculation showed a relative absorbed dose of 0.008 in slice 234 and in slice 269, respectively. Both slices are at a distance of $18 \times 0.36 \text{ cm} = 6.5 \text{ cm}$ from the center of the lesion, which is more than double the distances mentioned by the IAEA report. However, if one makes a similar calculation for the two-voxel air source mentioned in the previous section, then the 100 Gy isodose would appear at a distance of 3.2cm, which would agree with the IAEA data.

25 Gy was the surface absorbed dose reported in the IAEA document for the rim of the lesion at 10cm distance from the center. This corresponds to 28 slices of the MAX phantom, i.e. one has to look for the value of the relative absorbed dose in the surface voxels of slices 223 and 279. A relative absorbed dose of 0.003 was found in these slices, which corresponds to a surface voxel absorbed dose of $0.003 \times 12683 \text{ Gy} = 38 \text{ Gy}$ at 1.8mm depth, which is 50% greater than the value of the IAEA report. For the two-voxel air source a similar calculation gives 34 Gy at the rim of the lesion, which is still 36% greater than the IAEA value.

Figure 8 shows the area of the lesion defined by the ROI2 with indications of the maximum voxel absorbed dose (M), and various ranges for relative surface isodoses (B – F). The 0.008 isodose voxels (G) represent the 100 Gy isodose at 6.5cm from the center of the lesion.

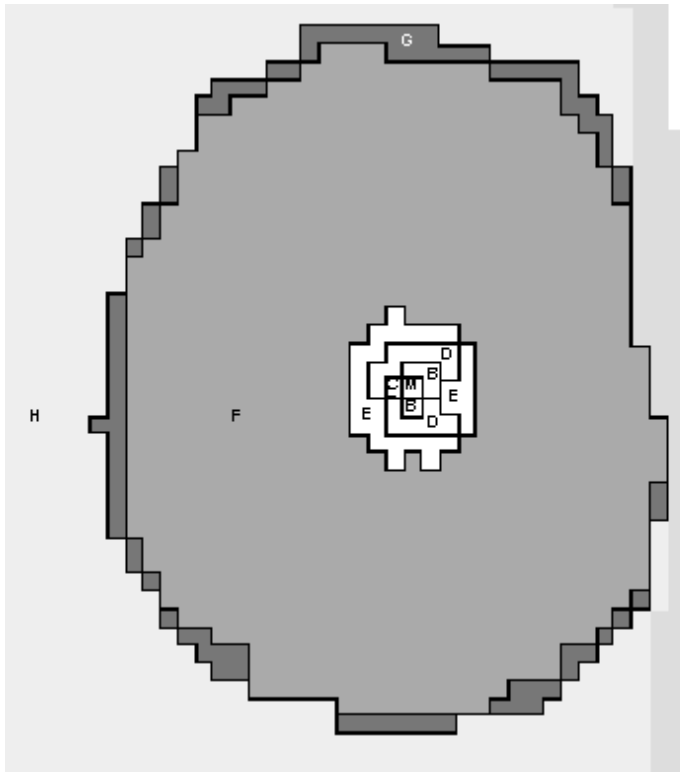


Figure 8. Surface isodoses for the absorbed dose distribution with SSD = 5.4mm
M = maximum voxel absorbed dose, Isodoses: B = 80-99%, C = 60-79%, D = 40-59%, E = 20-39%, F = 0.9-20%, G = 0.8% (100 Gy), H = 0.1-0.7%.

The maximum voxel absorbed dose of 12683 Gy corresponds to a depth of 1.8mm. If one extrapolates the iridium source depth dose in figure 5 to the surface, one gets a maximum surface absorbed dose of ca. 27850 Gy at zero depth. Analysis of the voxel absorbed depth doses at 6.5cm and at 10cm distance from the center of the lesion showed no difference between the value at 1.8mm depth and the extrapolated value at zero depth within the range given by the coefficient of variation, i.e. that the 100 Gy isodose and the 38 Gy isodose apply practically also to zero depth at 6.5cm and at 10cm distance, respectively. Extrapolation of the INEN depth dose in figure 5 gives a maximum surface absorbed dose of ca. 44180 Gy at zero depth.

3.4 Verification of the maximum surface absorbed dose

Because of the high activity of 1.37 TBq of the ¹⁹²Ir source, the very short SSDs, and the extreme exposure time of 6.5 hours the maximum surface absorbed dose of 27850 Gy does not come as a surprise. Nevertheless, just because in radiological accidents one often has to deal with high absorbed doses one would feel more confident about the results if they could be cross-checked with additional methods.

At the time of the accident the source activity was 1.37 TBq, which, based on the air kerma rate constant for ¹⁹²Ir, causes an air kerma rate of 0.167 Gy/h at 1m distance from the unshielded source, or 0.153 Gy/h at 1m distance from the encapsulated source. Assuming an ideal point source one can apply the inverse square law to make the following calculation:

For 3.5 h at 7mm distance: Air kerma = 0.153 Gy/h x (1000/7.0)² x □ 3.5 h = 10929 Gy

For 3.0 h at 3mm distance: Air kerma = 0.153 Gy/h x (1000/3.6)² x □ 3.0 h = 35417 Gy.

These results give a total air kerma of 46346 Gy, or taking into account the ratio between the mass energy absorption coefficients for soft-tissue and air, the total free-in-air soft-tissue kerma would be 51027 Gy at a distance of ca. 5.4mm. Simple considerations based on the exponential attenuation law show that the 0.36cm cotton layer produces a shielding effect of ca. 3% for the incident photon radiation, which reduces the total free-in-air soft-tissue kerma to 49496 Gy.

For a SSD of 5.4mm it is not possible to consider the 3.6mm x 3.6mm x 7.2mm two-voxel ¹⁹²Ir source as a point source. Therefore a comparative calculation with a SSD = 5.4mm has been made for a 3.6mm x 3.6mm x 7.2mm two-voxel air source on the one hand, and for a 1mm x 1mm x 1mm one-voxel air source on the other hand, which is still not a point source, but at least a better approximation to the ideal. The results show that the maximum voxel absorbed dose for the 1mm x 1mm x 1mm one-voxel air source is 2.21 times greater than the corresponding value for the 3.6mm x 3.6mm x 7.2mm two-voxel air source. Strictly spoken, this result does not apply directly to the real iridium source, but for the purpose of this assessment it is assumed that an iridium point source would also increase the maximum surface absorbed dose by about a factor of 2. This means, that the maximum surface absorbed dose would become ca. 27850 Gy x 2 = 55700 Gy, which differs from the total free-in-air soft-tissue kerma determined from the activity of the ¹⁹²Ir source by ca. 12.5%. This very rough assessment provides corroboration for the Monte Carlo results obtained.

3.5 Organ and tissue absorbed doses

Together with the calculation of the voxel absorbed dose distribution the Monte Carlo code also determines average absorbed doses to organs and tissues of the body, as well as the average whole body absorbed dose.

Table 3. Average organ and tissue absorbed doses calculated for the MAX phantom

Organ/Tissue	Average Dose
	[Gy]
Total Adipose	10.7
Pelvis	9.8
Total Skin	8.4
Total Muscle	8.1
Bladder	6.9
Whole body	6.4
Testes	6.0
Skeleton	4.2
Red bone marr.	4.1
Colon	2.8
Pancreas	0.5
Stomach	0.2
Lungs	0.1

Table 3 shows the results for a SSD = 5.4mm, i.e. for the exposure set-up representing the accidental irradiation. Average absorbed dose to the testes and the bladder are significantly smaller than the values given by the INEN in table 1. For the two-voxel air source these organ doses would be 10.4 Gy for the testes and 11.5 Gy for the bladder, which are still about only half of that what the INEN data indicate. Finally, with 6.4 Gy the average whole body absorbed dose found by the MAX/EGS4 exposure model is more than 5 times greater than the value determined by biological dosimetry.

One has to bear in mind that a point source close to the surface of one thigh represents a highly non-uniform irradiation of the body. For relatively small organs not too far away from the source, like the testes or the bladder, the average absorbed dose is approximately equal to the absorbed dose in all voxels of that organ. However, this assumption does not hold for extended organs and tissues, like adipose, muscle, skeleton, red bone marrow, skin, colon, and the whole body.

4. Conclusions

The simulation of the Yanango radiological accident with the MAX/EGS4 exposure model produced the following results:

- a) The maximum absorbed dose was calculated by Monte Carlo methods as 12683 Gy at 1.8mm depth in a surface voxel in front of the source, i.e. at the center of the lesion.
- b) The absorbed dose found at the entrance side of the femur was 178 Gy, and 101 Gy at the exit side.
- c) Based on the maximum voxel absorbed dose of 12683 Gy, the voxel isodose of 100 Gy was found at a distance of 6.5cm from the center of the lesion, and at 10cm distance the voxel isodose was found to be 38 Gy.
- d) Extrapolation of the voxel depth dose in the center of the lesion to zero depth gave a maximum surface absorbed dose of ca. 27850 Gy.
- e) Cross-checking the magnitude of the maximum surface absorbed dose by standard dosimetric methods confirmed the credibility of the Monte Carlo results.
- f) Average absorbed doses have been calculated for radiosensitive organs and tissues, as well as for the whole body.

Table 4. Summary of absorbed doses of the MAX/EGS4 Monte Carlo calculations, and of the IAEA Monte Carlo calculations, depth dose assessment, and biological dosimetry.

MC = Monte Carlo, SAD = Surface absorbed dose, biol.dos. = biological dosimetry

Quantity	MAX/EGS4	IAEA / MC	IAEA / INEN
Femur: entrance - exit	178 Gy - 101 Gy	15 Gy - 5 Gy	no data
Femur: average	140 Gy	10 Gy	143 Gy
100Gy surface isodose	6cm from center	2-3cm from center	no data
Isodose 10cm from center	38 Gy	25Gy	no data
Maximum SAD	27850 Gy	no data	44180 Gy
Testes absorbed dose	6.0 Gy	no data	23 Gy
Bladder absorbed dose	6.9 Gy	no data	18 Gy
Whole body absorbed dose	6.4 Gy	no data	1.25 Gy biol.dos.

Table 4 shows that between the results of this investigation and the IAEA data agreement can be found only for the average absorbed dose to the femur, although the data points for the INEN and the MAX/EGS4 results refer to different depths as figure 5 shows, and with some reservation for the

isodose 10 cm from the center, if one takes the 30% uncertainty of the IAEA/MC value into account. It was shown earlier that the 2-3cm distance of the 100 Gy isodose reported by the IAEA/MC calculations agrees with the MAX/EGS4 result only for a two-voxel air source. This would indicate a significant difference of the source modelling between the Monte Carlo calculations of the IAEA report and of this investigation. The same conclusion applies to the INEN depth dose data, because partial agreement with the MAX/EGS4 depth dose in figure 5 was found only for the two-voxel air source. Extrapolation of the INEN depth dose to the surface yielded ca. 44180 Gy for the center of the lesion, which is significantly greater than the maximum surface absorbed dose for the MAX/EGS4 model. Unfortunately no surface absorbed dose could be found for the Monte Carlo calculations in the IAEA report. Also, with an average absorbed dose of 10 Gy to the femur the IAEA/MC data are significantly smaller than the MAX/EGS4 and the IAEA/INEN results. Organ absorbed doses for the testes and the bladder show INEN values about three times greater than the MAX/EGS4 results, but on the other hand the IAEA whole body absorbed dose, determined by biological dosimetry, is only one fifth of the MAX/EGS4 whole body absorbed dose.

An explanatory discussion of agreements and disagreements remains difficult, because the IAEA report does not reveal sufficient details about the irradiation conditions used by the Peruvian physicist and by the French Monte Carlo team, but after all there are clear indications that the MAX/EGS4 simulations of the Yanango radiation accident produced reasonable results for the absorbed dose quantities presented.

Radiation physicians insist that early knowledge about the maximum absorbed dose, and about a comprehensive distribution of the absorbed dose in the body is of great importance for medical prognosis and choice of treatment. Physical dosimetry can provide various absorbed dose quantities, but it is up to the medical experts to decide which absorbed doses are most relevant for their decisions. The MAX/EGS4 exposure model can be considered a useful tool to calculate these quantities rapidly, and it can easily be modified to calculate voxel-specific absorbed dose distributions even within organs and tissues, if exposure conditions and/or medical considerations recommend doing so.

5. Acknowledgement

The authors would like to thank the Conselho Nacional de Desenvolvimento Científico e Tecnológico - CNPq and the Fundação de Amparo à Ciência do Estado de Pernambuco - FACEPE for the financial support. The authors would like to thank John Hunt, PhD from the IRD in Rio de Janeiro for his comments and especially Steve Seltzer, PhD from the NIST in Washington for his support.

6. References

- Borg J and Rogers D W O 1999 Spectra and air-kerma strength for encapsulated ¹⁹²Ir sources, *Med.Phys.* 26, No.11, pp 2441-2444
- Delacroix D, Guerre J P, Leblanc P and Hickman C 2002 Radionuclide and Radiation Protection Data Handbook 2002, *Rad.Prot.Dos.* Vol.98, No.1, pp 1-168
- Hubbell J H and Seltzer S M 1996 Stopping Powers and Ranges for Electrons, National Institute of Standards and Technology, <http://physics.nist.gov>
- IAEA 1998a Lessons to be learned from Accidents in Industrial Radiography, International Atomic Energy Agency, Safety Reports Series No.7, Vienna
- IAEA 1998b Diagnosis and Treatment of Radiation Injuries, International Atomic Energy Agency, Safety Reports Series No.2, Vienna
- IAEA 2000 The Radiological Accident in Yanango, International Atomic Energy Agency, Vienna
- ICRP 1991 1990 Recommendations of the International Commission on Radiological Protection. ICRP Publication 60. International Commission on Radiological Protection, Pergamon Press, Oxford

- ICRP 1995 Basic Anatomical and Physiological Data for use in Radiological Protection: The Skeleton. ICRP Publication 70. International Commission on Radiological Protection, Pergamon Press, Oxford
- ICRP 2003 Basic Anatomical and Physiological Data for Use in Radiological Protection: Reference Values. ICRP Publication 89, International Commission on Radiological Protection, Pergamon Press, Oxford
- Kramer R, Vieira J W, Khoury H J, Lima F R A and Fuelle D 2003 All About MAX: A Male Adult VoXel Phantom for Monte Carlo Calculations in Radiation Protection Dosimetry, *Phys. Med. Biol.*, 48, No.10, 1239-1262
- Kramer R, Vieira J W, Khoury H J, and Lima F R A 2004 MAX meets ADAM: A dosimetric comparison between a voxel-based and a mathematical model for external exposure to photons. *Phys. Med. Biol.* 49, 887-910
- Kramer R, Khoury H J, Vieira J W, Yoriyaz H and Lima F R A 2005a Effective Dose Ratios for Tomographic and Stylized Models from External Exposure to Photons. Paper presented at the Monte Carlo 2005 Topical Meeting. The Monte Carlo Method: Versatility Unbounded In A Dynamic Computing World", Chattanooga, TN, USA, April 17-21, 2005
- Kramer R, Khoury H J, Vieira J W, Loureiro E C M, Yoriyaz H and Lima F R A 2005b Effective Dose Ratios for Tomographic and Stylized Models from External Exposure to Electrons. Paper presented at the Monte Carlo 2005 Topical Meeting. The Monte Carlo Method: Versatility Unbounded In A Dynamic Computing World", Chattanooga, TN, USA, April 17-21, 2005
- Kramer R, Khoury H J, Vieira J W, Yoriyaz H, Loureiro E C M and LIMA F R A 2005c Effective Dose Ratios for Tomographic and Stylized Models from Internal Exposure to Electrons. Paper presented at the Monte Carlo 2005 Topical Meeting. The Monte Carlo Method: Versatility Unbounded In A Dynamic Computing World", Chattanooga, TN, USA, April 17-21, 2005
- Lima F R A, Kramer R, Khoury H J, dos Santos A M, Vieira J W 2005 Effective Dose Ratios for Tomographic and Stylized Models from Internal Exposure to Photons. Paper presented at the Monte Carlo 2005 Topical Meeting. The Monte Carlo Method: Versatility Unbounded In A Dynamic Computing World", Chattanooga, TN, USA, April 17-21, 2005
- Nelson W R, Hirayama H and Rogers D W O 1985 The EGS4 Code System, SLAC-265 Stanford Linear Accelerator Center, Stanford University, Stanford, California.
- NIST 2005 National Institute of Standards and Technology, Washington D.C., private communication: email from S.Seltzer from February 23, 2005
- Roux A, Bottolier-Depois J F and Gaillard-Lecanu E 2000 Qualifying Numerical Tools for Reconstructing Physical Doses in the Case of Accidental Exposure to Ionising Radiation, *Rad.Prot.Dos.*, Vol.87, No 4, pp 243-249
- Roux A, Gaillard-Lecanu E, Bottolier-Depois J F, Chau Q, Trompier F and Lebedev L 2001 Qualification of a Numerical Anthropomorphic Model Dedicated to Radiological Accidents, *Radioprotection*, Vol. 36, No.1, pp 57-75
- Zubal I G, Harrell C R, Smith E O, Rattner Z, Gindi G, Hoffer P B 1994 Computerized three-dimensional segmented human anatomy, *Med.Phys.* 21 No.2, 299-302